

Research Article

Parameters of Porosity and Compressive Strength-Based Optimization on Reinforced Aluminium from the Recycled Waste Automobile Frames

A. Parthiban,¹ V. Vijayan ,² T. Sathish ,³ S. Dinesh Kumar,⁴ L. Ponraj Sankar,⁵
N. Parthipan,⁶ Dawit Tafesse ,⁷ and Mebratu Tufa ⁷

¹Department of Mechanical Engineering, Vels Institute of Science Technology & Advanced Studies, Pallavaram, Chennai 600 117, Tamil Nadu, India

²Department of Mechanical Engineering, K. Ramakrishnan College of Technology (Autonomous), Samayapuram, Trichy 621 112, Tamil Nadu, India

³Department of Mechanical Engineering, Saveetha School of Engineering, SIMATS, Chennai 602 105, Tamil Nadu, India

⁴Department of Mechanical Engineering, St. Peter's Institute of Higher Education and Research, Avadi, Chennai 600 054, Tamil Nadu, India

⁵Department of Civil Engineering, CMR Institute of Technology, Hyderabad, India

⁶Department of Mechanical Engineering, M. Kumarasamy College of Engineering, Karur, Tamil Nadu, India

⁷Department of Mechanical Engineering, Faculty of Manufacturing, Institute of Technology, Hawassa University, Hawassa, Ethiopia

Correspondence should be addressed to T. Sathish; sathish.sailer@gmail.com and Dawit Tafesse; dawitt@hu.edu.et

Received 25 June 2021; Revised 22 July 2021; Accepted 16 October 2021; Published 8 November 2021

Academic Editor: Samson Jerold Samuel Chelladurai

Copyright © 2021 A. Parthiban et al. This is an open access article distributed under the Creative Commons Attribution License, which permits unrestricted use, distribution, and reproduction in any medium, provided the original work is properly cited.

Automobile industries were ready to recycle the waste old parts as well as the damaged parts of the old vehicles as much as possible. This study mainly focused on the recycling of the waste and damaged aluminium frames of the automobile bodies. These aluminium-based frames only collected the metal matrix composite created by reinforcement of 3% silicon carbide (SiC) and 3% high carbon steel. The stir casting method is chosen to make the composites. Optimization is done by Taguchi ANOVA technique. Three input parameters such as stir speed, time of squeeze, and the temperature of the preheating were considered. The outputs such as compressive strength and porosity were experimentally measured with the combination of nine (L9) experimental trails. The measured experimental results were analyzed and optimized with the help of Taguchi technique with different plots for clear identification. The optimized parameters based on low porosity and high compressive strength were recommended for conclusion.

1. Introduction

Nowadays, recycling the wastes is considered as the new production in the industrial world. In automobile industry, arrival of the new vehicles leads to increasing old vehicle scraps. Krishnan et al. [1] entirely studied about scrap of aluminium-used composites' metal matrix. The source aluminium is clearly collected and used from the wastes. They provide explanation and accomplishment suggestion concerning different methods bringing into play for creation

through those wastes as well as scraps. Furthermore, they explained the various composite material microstructure behavior and composite material mechanical properties with various experiment results.

Similarly, Gupta and Satyanarayana [2] completely discussed the solidification procedure on metal matrix composites of aluminium with the help of various researchers point of view. There are different methods, processes, combination of composite materials and corresponding parameters considered, and optimization

methods used for the metal matrix. They also mentioned individually in a clear manner. Gesing and Wolanski [3], without a doubt, argued on the subject of recycling the light metals from the used vehicles and spare parts of the automobiles and scraps. These suggestions afford assurance to generate research work related to this method.

Christy et al. [4] discussed the stir and squeeze casting input parameters optimization by using the technique of Taguchi with four different input and outputs for the experiments. They express the microstructures to identify the relation of the experimental result outcomes. They used the aluminium alloy wheel scrap for the formation of the composites by the method of stir casting. They optimized with help of the Taguchi method based on the preferable mechanical properties' outcomes and also explained them with optical microscopic images, scanning electron microscopic images, and diffraction of X-ray and X-ray spectroscopy. Importance of the porosity was explained.

The fundamental belongings to the optimization method for different reinforced composites such as Al reinforced to nanomaterials [5], Al reinforced to ZrC [6], and Al reinforced to silicon carbide [7] were discussed clearly. In the same way, various operations such as turning process [8], diffusion bonding [9], laser welding process [10], electrochemical machining [11], and A-GTAW welding [12] were experimentally tried in each article with different parameters and responses.

Mazahery and Shabani [13] undoubtedly investigated the composites of sintered Al matrix regarding the abrasive wear behavior and microstructure property with various experiments and clear comparison on results. Dai et al. [14] explained about the aluminium scrap details and aluminium content based on recycling and also expressed about the fibers of carbon materials. They also mentioned that the scrap of the aluminium material-based car parts was increased day by day due to the need of the increasing vehicles with different articles' reference.

Cullen and Allwood [15] explained about liquid aluminium-based product conversion into global usages. They created the recycled secondary products of aluminium by using the ancient scraps of aluminium collected from different places of the customers. They used recycling in the closed loop method. Oliveux et al. [16] reviewed various articles regarding the reinforcement of composites with various methods. They mentioned about the reuse and recycling of different composites.

Mishra and Srivastava [17] explained about the wear behavior of the composite of aluminium alloy with silicon carbide with the number of SEM images with respect to the load variation. They clearly mentioned the microstructures of the composites. Almadhoni and Khan [18] reviewed the metal matrix composite research article with different combinations and different compositions of various metals. They mainly focused the stir casting process with three major parameters such as temperature of the die and speed of the stirrer. They also conclude that the speed of the stirrer is directly proportional to the homogenous collaboration on the reinforcement matrix of aluminium alloys.

Chandla et al. [19] reviewed the stir casting process with the aluminium alloy-based composites. They mainly listed the various combinations of materials such as alumina, silicon carbide, barium carbide, red mud, iron oxide, aluminium oxide, frit, graphite, carbon nano tube, zirconium oxide titanium carbide, and other materials in different percentage volumes with aluminium alloy-based composites. They compared the considered parameter variations and mentioned the corresponding properties augmentations for single metal matrix composites and hybrid composite metal matrix. Silicon carbide-based stir casting parameters are also compared with their consequences.

Arulraj et al. [20], Manivannan and Sasikumar [21], M. K. Sahu and R. K. Sahu [22], and Aravindan et al. [23] clearly explained the following. Stir casting method retains numerous benefits over further conventional techniques such as less handling cost, high homogeneity between the particulates, absorption of moisture is low, and suitable for huge manufacture. It is also preferable for different sizes with various shapes and dimensions. Due to its simple method for the production, it is the most preferable one for the production industry. This can be used to reduce the cost of the production from 10% to 35% of the other methods used for production.

In this paper, reinforced composite was created from the waste automobile frames by recycling along with reinforcement materials such as silicon carbide and high carbon steel. These composite specimens were prepared by the stir casting method. The suitable stir casting parameters will be selected based on properties such as porosity and compressive strength by the optimization method.

1.1. Experimental Procedure. From the automobile industries, automobile service centres, and mechanic workshops, the samples of the aluminium frames were collected and converted into small scrap pieces. The scraps of aluminium having composition such as 0.95% of magnesium, 0.7% of silicon, 0.68% of iron, 0.39% of copper, 0.31% of zinc, 0.16% of manganese, 0.2% of titanium, and 0.4% of chromium, and then, the remaining have aluminium content in the percentage of weight basis. There is 92% of scrap particles reinforcement with two materials for the remaining percentage of volume concentrations.

There is 3% of silicon carbide, and the remaining 3% is utilized with the high carbon steel. All these materials were in the form of powder. The scrap aluminium material is powered by using the ball bearing pulveriser. Then, these materials were placed into the stir casting machine. This stir casting has the pouring method in the bottom side. The machine shown in Figure 1 has the electrical furnace, reinforcement preheating chamber, runway preheater, hydraulic sequence pressure ram, and electrical control panel.

In this optimization-based investigation, L9 ANOVA table is used as per Table 1. It contains variations in holding temperature which were 300°C, 400°C, and 500°C. The squeezing time considered were 20 sec deviation from the 20 sec to 60 sec. Then, the stir speed is maintained with 100 rpm variation starting with 400 rpm to 600 rpm. The holding pressure is



FIGURE 1: Stir casting machine.

TABLE 1: Details of experimental parameters (L9).

Trail of experiment no.	Holding temperature as temp (°C)	Time as t in sec	Stir speed as N in rpm
TE 1	300	20	400
TE 2	300	40	500
TE 3	300	60	600
TE 4	400	20	500
TE 5	400	40	600
TE 6	400	60	400
TE 7	500	20	600
TE 8	500	40	400
TE 9	500	60	500

maintained as 120 MPa throughout the process. The specimens were prepared for both desired properties such as porosity and compressive strength with the dimensions of 40 mm diameter and 30 mm height in small cylinders.

The porosity of the specimens was calculated with the traditional formula that if the ratio of the experimental and theoretical density values was multiplied by 100, then the total value is subtracted from the number one. By Archimedes principle, the experimental density of the individual sample specimen is obtained. Similarly, the theoretical density is obtained from the rule of the mixture on the specimen. Then, the compressive strength is measured by the traditional method in a universal testing machine with compressive strength analyzed as per the ASTM standards such as ASTM E9. Porosity and compressive strength of the individual specimen was tested as per Table 1.

2. Results and Discussion

2.1. Porosity. The experimentally measured values of porosity and the compressive strength are mentioned in Table 2

TABLE 2: Experimental results for the trails of experiments.

Trail of experiment no.	Porosity in %	Compressive strength CS in MPa
TE 1	12.328	319.44
TE 2	18.215	345.58
TE 3	24.102	371.72
TE 4	12.155	306.34
TE 5	18.042	332.48
TE 6	22.948	360.72
TE 7	11.982	293.24
TE 8	16.888	321.48
TE 9	22.775	347.62

in detail. There are nine trials which were conducted as per Table 1. Initially, porosity-based results were examined with minimum being the desirable condition. Then, the compressive strength was examined with maximum being the desirable condition. Then, both porosity and compressive strength values were examined with nominal being the suitable condition. All these three examinations were conducted with the help of the Taguchi analysis by using the Minitab 18 software.

Significant consequence diagram based on the SN ratio for experimental results of porosity is clearly mentioned in Figure 2. In this place, minimum porosity in needed condition is used. Significantly minimum results of porosity can be obtained at 500°C of the holding temperature with 20 sec of the holding time and 400 rpm speed of the stir in the stir casting process. Likewise, the significant consequence diagram based on the means of porosity is shown in Figure 3. The maximum porosity is obtained at the input parameters such as 300°C of the holding temperature with 60 sec of the holding time and 600 rpm speed of the stir. From these two diagrams, minimum and maximum porosity obtaining parameters were clearly obtained.

Comparison of porosity responses using contour plots is shown in Figure 4. There are three different contour plots such as time in competition with temperature, speed contrasted with temperature, and speed versus time available based on the porosity results. The variations on the contour plot were expressed in the form of the colour variation with the various ranges for the individual colours based on the intensity of the experimental results achieved from the experiments. Similarly, Figure 5 shows the surface plots comparison for porosity as the three-in-one diagram. In this diagram, porosity in the vertical direction and the remaining two directions in each diagram are time-contrasted with temperature, speed as opposed to temperature, and speed in competition with time, respectively.

Significant consequence table for porosity is clearly mentioned in Table 3 for both SN ratio and means response. The highest priority of the parameters reached as rank of one, two and three for the holding time, stir speed, and holding temperature in the same order. So, the holding time has the superior contribution when compared to other similar speed of the stir which has the least significant contribution based on the minimum porosity outcomes. The corresponding regression equation is given as follows for the considered parameter-based experimental results:

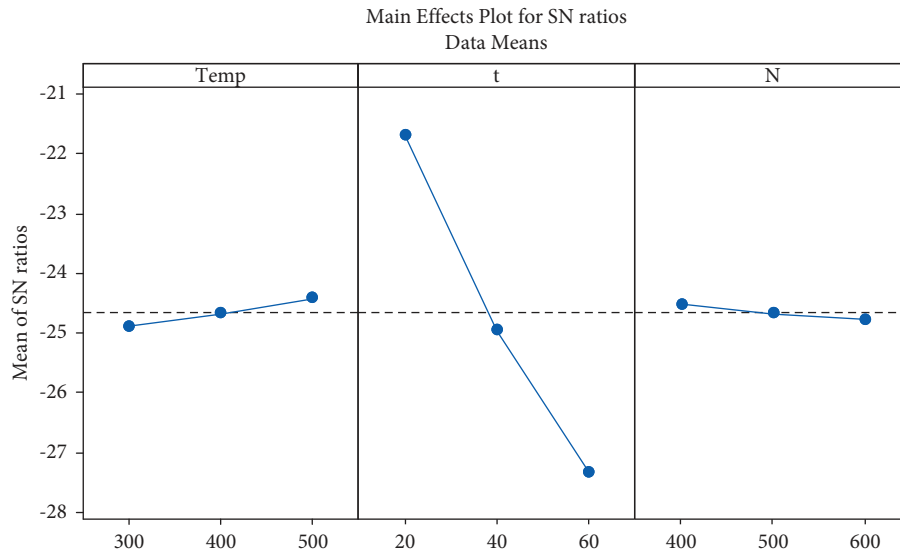


FIGURE 2: Significant consequence diagram based on the SN ratio for porosity (temp: temperature in °C; *t*: time in sec; and *N*: stir speed in rpm).

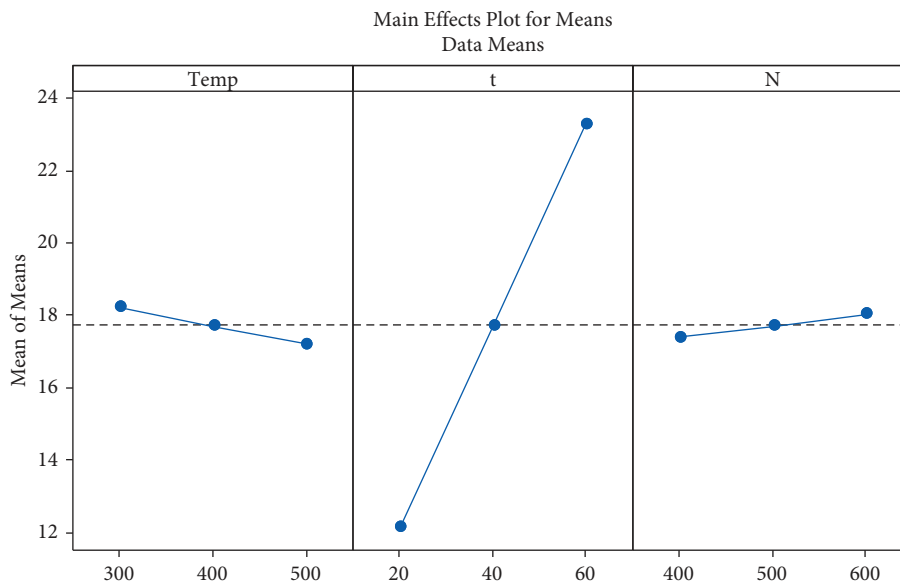


FIGURE 3: Significant consequence diagram based on means for porosity (temp: temperature in °C; *t*: time in sec; *N*: stir speed in rpm).

regression equation for porosity

$$= 6.960 - 0.005000 \text{ temp} + 0.2780 t + 0.003270 N. \quad (1)$$

2.2. *Compressive Strength.* Significant consequence diagram based on the SN ratio for compressive strength is evidently pointed out in Figure 5. Similarly, Figure 6 explains about the significant consequence diagram based on means for compressive strength. These two figures were supported each other with the same condition such that the greatest compressive strength is preferable. These two figures based on the experimental outcomes of the compressive strength results obviously point out that the uppermost compressive strength is obtained for the input parameters such as 300°C

of the holding temperature with 60 sec of the holding time and 400 rpm speed. Likewise, the lowest compressive strength is obtained for the input parameters such as 500°C of the holding temperature with 20 sec of the holding time and 600 rpm of stir speed of the stir in the friction stir operation.

Figure 7 unmistakably shows the contour plots comparison such as speed with respect to temperature, time with respect to temperature, and speed with respect to time for the compressive strength results with different colour intensities for different range of results in Figure 8. Similarly, Figure 9 demonstrates the surface plots comparison such as compressive strength in vertical axis and horizontal axis which were mentioned with speed versus temperature, time versus temperature, and speed versus time. Table 3 provides

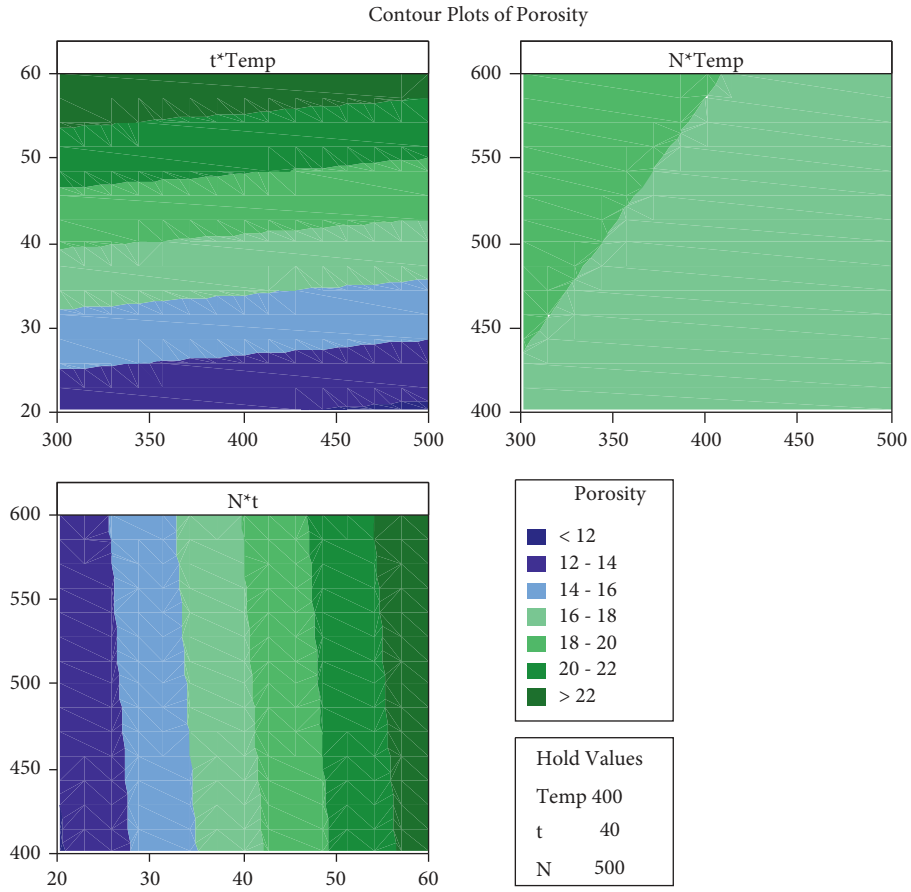


FIGURE 4: Contour plots comparison for porosity (temp: temperature in °C; t : time in sec; N : stir speed in rpm).

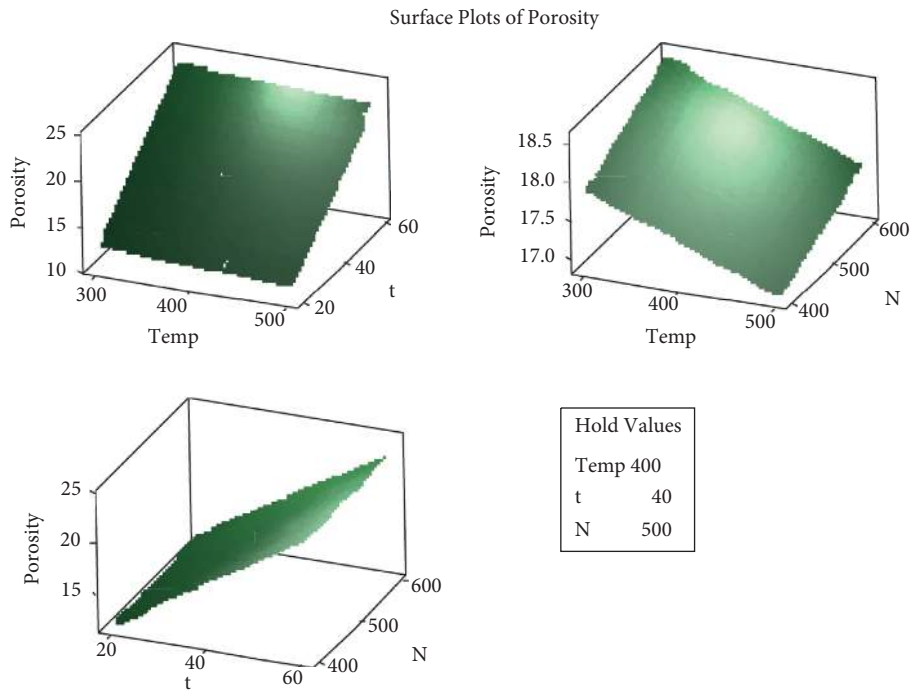


FIGURE 5: Comparison of surface plots for porosity (temp: temperature in °C; t : time in sec; N : stir speed in rpm).

TABLE 3: Significant consequence for porosity.

Level	Response for SN ratio			Response for means		
	Temperature (°C)	Time (sec)	Stir speed (rpm)	Temperature (°C)	Time (sec)	Stir speed (rpm)
1	-24.89	-21.69	-24.53	18.22	12.15	17.39
2	-24.68	-24.96	-24.68	17.72	17.72	17.72
3	-24.42	-27.34	-24.78	17.22	23.28	18.04
Delta	0.47	5.64	0.25	1.00	11.12	0.65
Rank	2	1	3	2	1	3

Temp: temperature in °C; t: time in sec; N: stir speed in rpm

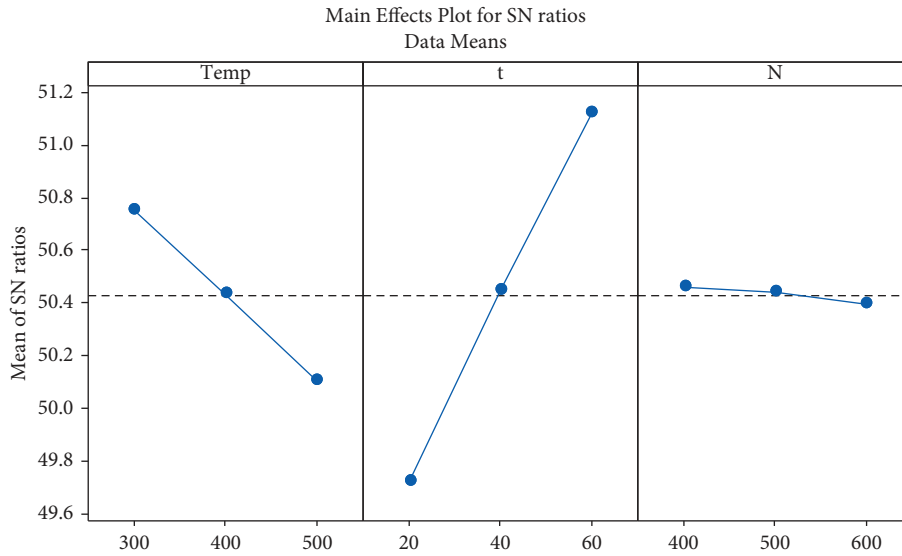


FIGURE 6: Significant consequence diagram based on the SN ratio for compressive strength (temp: temperature in °C; t: time in sec; N: stir speed in rpm).

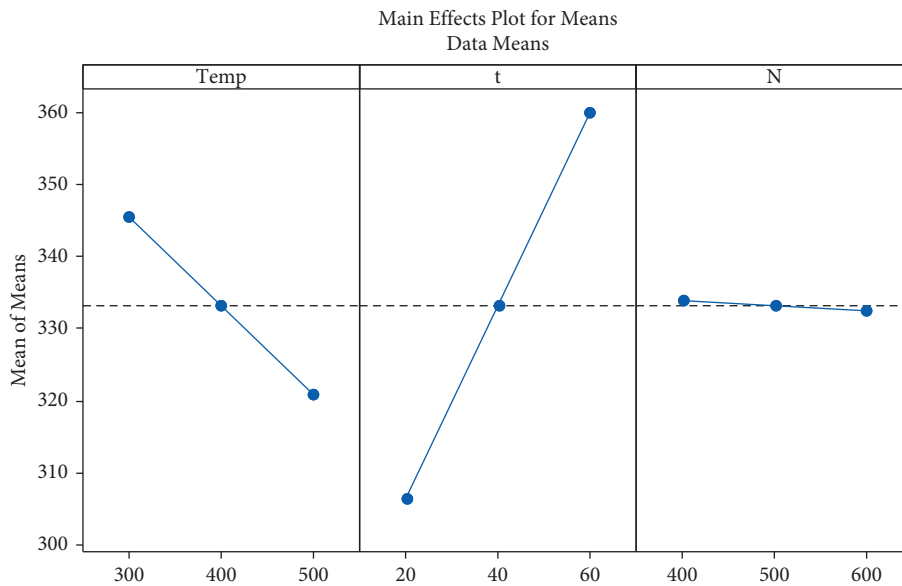


FIGURE 7: Significant consequence diagram based on means for compressive strength (temp: temperature in °C; t: time in sec; N: stir speed in rpm).

the response of the compressive strength based on SN ratio and means. Here, larger is better condition is used. The first, second, and third ranks are provided for time, holding

temperature, and stir speed, respectively and the corresponding regression equation is mentioned as follows for the compressive strength based on the input parameters used:

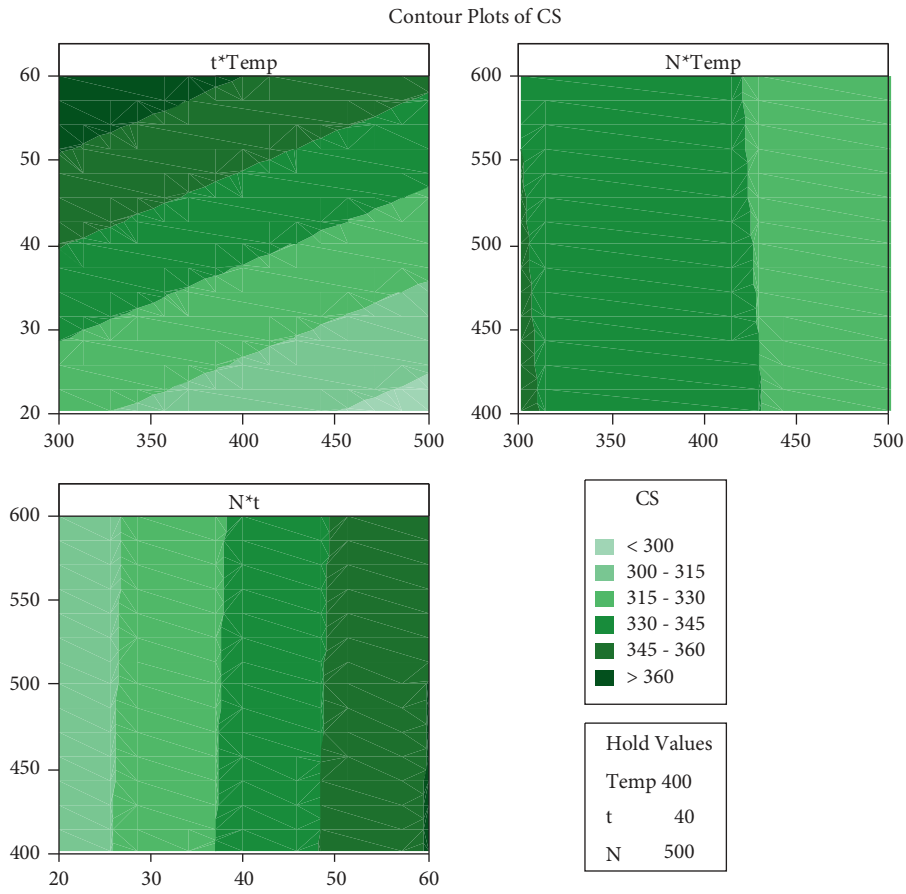


FIGURE 8: Comparison of the compressive strength using contour plots (temp: temperature in °C; t: time in sec; N: stir speed in rpm).

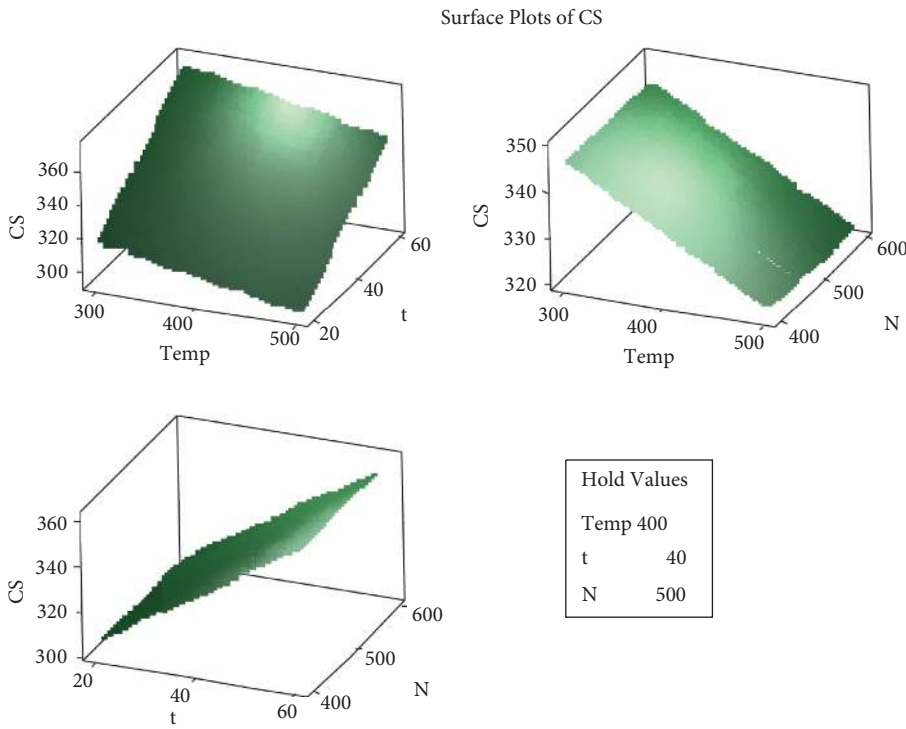


FIGURE 9: Comparison of the compressive strength using surface plots (temp: temperature in °C; t: time in sec; N: stir speed in rpm).

TABLE 4: Porosity and compressive strength-based responses.

Level	Temperature (°C)	Time (sec)	Stir speed (rpm)
1	-47.28	-46.36	-46.99
2	-46.95	-46.96	-46.96
3	-46.62	-47.53	-46.91
Delta	0.66	1.18	0.08
Rank	2	1	3

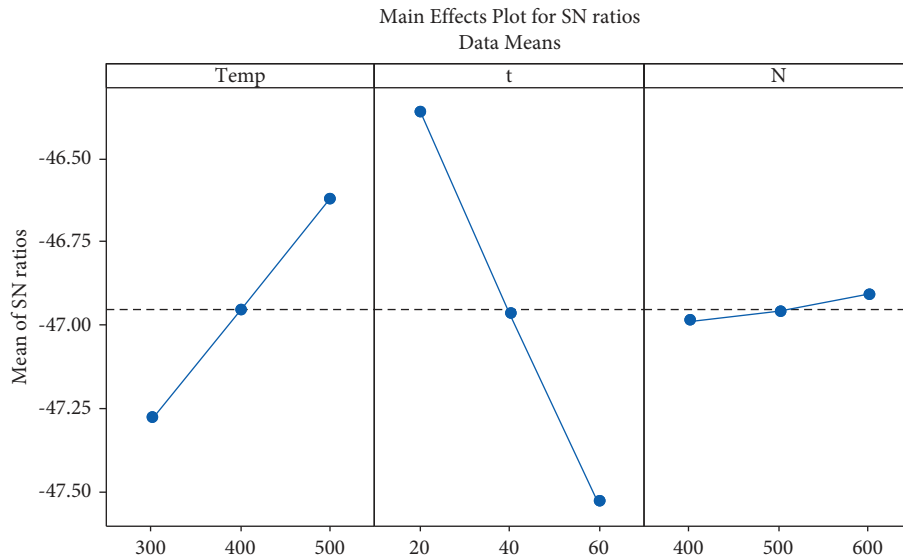


FIGURE 10: Significant consequence diagram based on the SN ratio for porosity and compressive strength (temp: temperature in °C; t: time in sec; N: stir speed in rpm).

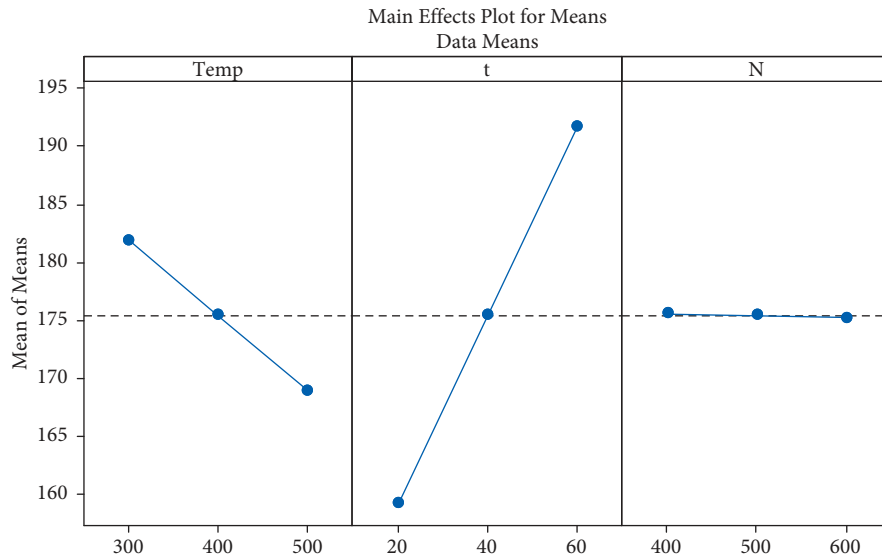


FIGURE 11: Significant consequence diagram based on means for porosity and compressive strength (temp: temperature in °C; t: time in sec; N: stir speed in rpm).

regression equation for compressive strength
 $= CS = 332.6 - 0.1240 \text{ temp} + 1.342 t - 0.007000 N.$

(2)

2.3. Porosity and Compressive Strength. After completing the individual optimization based on porosity and compressive strength values, the combination of these two was considered with nominal being the best condition in Table 4.

TABLE 5: Compressive strength response table.

Level	Response for SN ratio			Response for means		
	Temperature (°C)	Time (sec)	Stir speed (rpm)	Temperature (°C)	Time (sec)	Stir speed (rpm)
1	50.75	49.72	50.46	345.6	306.3	333.9
2	50.43	50.45	50.44	333.2	333.2	333.2
3	50.10	51.12	50.39	320.8	360.0	332.5
Delta	0.65	1.40	0.06	24.8	53.7	1.4
Rank	2	1	3	2	1	3

Figure 10 shows the significant consequence diagram based on the SN ratio for porosity and compressive strength. Similarly, Figure 11 shows the significant consequence diagram based on means for porosity and compressive strength. From Figures 10 and 11, the nominal results can be achieved for the input parameters such as 500°C of the holding temperature with 20 sec of the holding time and 600 rpm speed of the stir. Table 5 provides the porosity and compressive strength-based responses with the ranks such as first rank for time, second rank for holding temperature, and last rank for stir speed. Time is superior and most important parameter for porosity and compressive strength. Among these three cases, speed of stir obtained the very low preference for the responses.

3. Conclusion

This study on parameters of porosity and compressive strength-based optimization on reinforced aluminium from the recycled waste automobile frames can be possible, and the corresponding conclusions are as follows:

- (i) The lowest porosity-based optimum parameters were 500°C of holding temperature with 20 sec of holding time and 400 rpm speed of the stir
- (ii) The maximum compressive strength-based optimum parameters were 300°C of holding temperature with 60 sec of holding time and 400 rpm speed of the stir
- (iii) The porosity and compressive strength-based optimum parameters were 500°C of holding temperature with 20 sec of holding time and 600 rpm speed of the stir
- (iv) In future, the work was extended to conduct the impact test for checking the impact strength of the frame in the vehicle and also planned to conduct the corrosion test of the reinforced composites

Data Availability

The data used to support the findings of this study are included in the article. Further data or information which are required are available from the corresponding author upon request.

Disclosure

This work was performed as a part of the Employment Hawassa University, Ethiopia.

Conflicts of Interest

The authors declare that there are no conflicts of interest regarding the publication of this paper.

Acknowledgments

The authors appreciate the support from Hawassa University, Ethiopia. The authors thank Saveetha School of Engineering, SIMATS, Saveetha University, Chennai, Tamil Nadu, India, for the Technical Assistance to complete this experimental work.

References

- [1] P. K. Krishnan, J. V. Christy, R. Arunachalam et al., "Production of aluminum alloy-based metal matrix composites using scrap aluminum alloy and waste materials: influence on microstructure and mechanical properties," *Journal of Alloys and Compounds*, vol. 784, pp. 1047–1061, 2019.
- [2] N. Gupta and K. G. Satyanarayana, "Symposium review: solidification processing of MMCs," *Journal of Materials Science*, vol. 58, no. 6, pp. 91–93, 2006.
- [3] A. Gesing and R. Wolanski, "Recycling light metals from end-of-life vehicle," *Journal of the Minerals Metals & Materials Society*, vol. 53, no. 11, pp. 21–23, 2001.
- [4] J. V. Christy, R. Arunachalam, A.-H. I. Mourad et al., "Processing, properties, and microstructure of recycled aluminum alloy composites produced through an optimized stir and squeeze casting processes," *Journal of Manufacturing Processes*, vol. 59, pp. 287–301, 2020.
- [5] T. Sathish, K. Muthukumar, R. Saravanan, and V. Dhinakaran, "Study on temperature difference of aluminium nitride nanofluid used in solar flat plate collector over normal water," *AIP Conference Proceedings*, vol. 2283, no. No. 1, Article ID 020126, 2020.
- [6] T. Sathish and N. Sabarirajan, "Synthesis and optimization of AA 7175 - Zirconium Carbide (ZrC) composites machining parameters," *Journal of New Materials for Electrochemical Systems*, vol. 24, no. 1, pp. 34–37, 2021.
- [7] T. Sathish, N. Sabarirajan, and S. Karthick, "Machining parameters optimization of Aluminium Alloy 6063 with reinforcement of SiC composites," *Materials Today: Proceedings*, vol. 33, pp. 2559–2563, 2020.
- [8] S. P. Palaniappan, K. Muthukumar, R. V. Sabariraj, S. Dinesh Kumar, and T. Sathish, "CNC Turning process parameters optimization on Aluminium 6082 alloy by using Taguchi and ANOVA," *Materials Today: Proceedings*, vol. 21, pp. 1013–1021, 2020.
- [9] T. Sathish, S. Dinesh Kumar, K. Muthukumar, and S. Karthick, "Temperature distribution analysis on diffusion bonded joints of Ti-6Al-4V with AISI 4140 medium carbon

- steel,” *Materials Today: Proceedings*, vol. 21, pp. 847–856, 2020.
- [10] T. Sathish, P. Sevel, P. Sudharsan, and V. Vijayan, “Investigation and optimization of laser welding process parameters for AA7068 aluminium alloy butt joint,” *Materials Today: Proceedings*, vol. 37, pp. 1672–1677, 2021.
- [11] T. Sathish, “Experimental investigation of machined hole and optimization of machining parameters using electrochemical machining,” *Journal of Materials Research and Technology*, vol. 8, no. 5, pp. 4354–4363, 2019.
- [12] T. Sathish, S. Dinesh Kumar, K. Muthukumar, and S. Karthick, “Natural inspiration technique for the parameter optimization of A-GTAW welding of naval steel,” *Materials Today: Proceedings*, vol. 21, pp. 843–846, 2020.
- [13] A. Mazahery and M. O. Shabani, “Study on microstructure and abrasive wear behavior of sintered Al matrix composites,” *Ceramics International*, vol. 38, no. 5, pp. 4263–4269, 2012.
- [14] Q. Dai, J. Kelly, and A. Elgowainy, “Material efficiencies and recycling of aluminum and carbon fiber reinforced plastics for automotive applications,” *Energy Syst*, vol. 2, pp. 1–10, 2016.
- [15] J. M. Cullen and J. M. Allwood, “Mapping the global flow of aluminum: from liquid aluminum to end-use goods,” *Environmental Science & Technology*, vol. 47, no. 7, pp. 3057–3064, 2013.
- [16] G. Oliveux, L. O. Dandy, and G. A. Leeke, “Current status of recycling of fibre reinforced polymers: review of technologies, reuse and resulting properties,” *Progress in Materials Science*, vol. 72, pp. 61–99, 2015.
- [17] A. K. Mishra and R. K. Srivastava, “Wear behaviour of Al-6061/SiC metal matrix composites,” *Journal of the Institution of Engineers: Series C*, vol. 98, no. 2, pp. 97–103, 2017.
- [18] K. Almadhoni and S. Khan, “Review of effective parameters of stir casting process on metallurgical properties of ceramics particulate Al composites,” *IOSR Journal of Mechanical and Civil Engineering*, vol. 12, no. 6, pp. 22–40, 2015.
- [19] N. K. Chandla, S. Kant, and M. M. Goud, “Mechanical, tribological and microstructural characterization of stir cast Al-6061 metal/matrix composites-a comprehensive review,” *Sādhanā*, vol. 46, no. 1, pp. 1–38, 2021.
- [20] M. Arulraj, P. K. Palani, and L. Venkatesh, “Optimization of process parameters in stir casting of hybrid metal matrix (LM25/SiC/B4C) composite using taguchi method,” *Journal of Advances in Chemistry*, vol. 13, no. 9, pp. 6475–6479, 2017.
- [21] A. Manivannan and R. Sasikumar, “Exemplary encapsulate feeding in stir casting for quality composites,” *Materials and Manufacturing Processes*, vol. 34, no. 6, pp. 689–694, 2019.
- [22] M. K. Sahu and R. K. Sahu, “Fabrication of aluminum matrix composites by stir casting technique and stirring process parameters optimization,” in *Advanced Casting Technologies* IntechOpen, London, UK, 2018.
- [23] S. Aravindan, P. V. Rao, and K. Ponappa, “Evaluation of physical and mechanical properties of AZ91D/SiC composites by two step stir casting process,” *Journal of Magnesium and Alloys*, vol. 3, no. 1, pp. 52–62, 2015.